

Fermi surface of LaRu₄P₁₂: A clue to the origin of the metal-insulator transition in PrRu₄P₁₂S. R. Saha,^{1,*} H. Sugawara,^{1,†} Y. Aoki,¹ H. Sato,¹ Y. Inada,^{2,‡} H. Shishido,² R. Settai,² Y. Ōnuki,^{2,§} and H. Harima³¹*Department of Physics, Tokyo Metropolitan University, Hachioji, Tokyo 192-0397, Japan*²*Department of Physics, Osaka University, Toyonaka, Osaka 560-0043, Japan*³*Department of Physics, Kobe University, Nada, Kobe 657-8501, Japan*

(Received 17 October 2004; revised manuscript received 27 December 2004; published 7 April 2005)

We report the de Haas–van Alphen (dHvA) effect and magnetoresistance in the filled-skutterudite superconductor LaRu₄P₁₂, which is a reference material of PrRu₄P₁₂ that exhibits a metal-insulator (M-I) transition at $T_{MI} \approx 60$ K. The observed dHvA branches for the main Fermi surface (FS) are well explained by the band-structure calculation, using the full potential linearized augmented-plane-wave method with the local-density approximation, suggesting a nesting instability with $\mathbf{q}=(1,0,0)$ in the main multiply connected FS as expected also in PrRu₄P₁₂. Observed cyclotron effective masses of $(2.6-11.8)m_0$, which are roughly twice the calculated masses, indicate the large mass enhancement even in the La-skutterudites. Comparing the FS between LaRu₄P₁₂ and PrRu₄P₁₂, an essential role of *c-f* hybridization cooperating with the FS nesting in driving the M-I transition in PrRu₄P₁₂ is clarified.

DOI: 10.1103/PhysRevB.71.132502

PACS number(s): 75.20.Hr, 75.30.Mb, 71.18.+y, 71.27.+a

The filled-skutterudite compounds $R\text{Tr}_4\text{Pn}_{12}$ (R = rare earth; $\text{Tr}=\text{Fe, Ru, Os}$; and $\text{Pn}=\text{pnictogen}$) have attracted much attention¹ for exhibiting novel physical properties, i.e., metal-insulator (M-I) transition,² unconventional superconductivity,^{3,4} semiconducting behavior,^{5,6} magnetic ordering,⁵ and their prospect in thermoelectric applications.¹ Particularly interesting are Pr-based skutterudites, in which quadrupolar interactions are believed to play an important role for the anomalous properties.^{3,6-9} PrRu₄P₁₂ shows an exotic M-I transition at $T_{MI} \approx 60$ K,² probably with a non-magnetic origin, as suggested by no anomaly in the magnetic susceptibility (χ) and no essential effect of the magnetic field on the specific-heat anomaly up to 12 T.^{2,10} Although several studies have been carried out,^{2,10-14} the mechanism of the M-I transition remains one of the most mysterious puzzles in the skutterudites.

From the band-structure calculation,¹⁵⁻¹⁷ Harima has suggested that the M-I transition could be triggered by the nearly perfect nesting of the main Fermi surface (FS) with $\mathbf{q}=(1,0,0)$; the shape of the main FS is nearly cubic and its volume is one-half of the body-centered-cubic (bcc) Brillouin zone (BZ). Actually, both the electron¹¹ and the x-ray^{12,13} diffraction experiments have revealed a doubling of the unit-cell volume across T_{MI} ; it is suggested that the structure changes from bcc ($Im\bar{3}$) to simple cubic ($Pm\bar{3}$), caused by the different shift of Ru and P ions around two adjacent Pr ions, i.e., between the corner and body-centered Pr ion sites in bcc structure. However, the predicted distortion of the P ion to obtain an insulating band structure is much larger than that experimentally determined by the x-ray diffraction.^{12,17,18} If the *4f* electrons in PrRu₄P₁₂ are localized, as indicated by the Curie-Weiss behavior of χ ,² or only weakly hybridize with conduction electrons, then the electronic structure is expected to be basically the same as the reference material LaRu₄P₁₂, which shows a superconducting transition at $T_C \approx 7$ K,¹⁹ without a *4f* electron. In that case, LaRu₄P₁₂ is also expected to have the same nesting instability, however no M-I transition has been reported. Thus, it is essentially important to clarify the FS of both

compounds experimentally to understand the origin of the M-I transition in PrRu₄P₁₂. However, the high transition temperature of $T_{MI} \approx 60$ K prevents the observation of dHvA oscillations in the metallic state of PrRu₄P₁₂. As an alternative way, the experimental determination of FS in LaRu₄P₁₂ should be useful to understand the origin of the M-I transition in PrRu₄P₁₂, if it is carefully compared with the computed FSs of the two compounds based on the band-structure calculation.

We have succeeded in growing high-quality single crystals of LaRu₄P₁₂ and in observing the dHvA effect, the preliminary result of which has been briefly reported in Ref. 20. In this paper, we report the detailed experimental results on the dHvA effect and magnetoresistance along with the band-structure calculation in LaRu₄P₁₂, followed by a discussion on the possible origin of the M-I transition in PrRu₄P₁₂.

Single crystals of LaRu₄P₁₂ were grown by the tin-flux method, which is basically the same as described in Ref. 5. The raw materials were 4N (99.99% pure) -La, -Ru, 6N-P, and 5N-Sn. The residual resistivity ratio (RRR) of the present sample is about 700, indicating the high sample quality. The dHvA experiments were performed in a top loading ³He cryostat down to 0.4 K with a 15 T superconducting (SC) magnet and a top loading dilution refrigerator cooled down to ~ 30 mK with a 17 T SC magnet. The dHvA signals were detected by means of the conventional field modulation method with a low frequency ($f \sim 10$ Hz). The magnetoresistance was measured by the dc four-probe method using a top loading ³He cryostat equipped with a 16 T SC magnet.

Figure 1 shows (a) a typical recorder trace of the dHvA oscillations and (b) the corresponding fast Fourier transformation (FFT) spectra in LaRu₄P₁₂ at 31 mK for the magnetic field (H) along the $\langle 111 \rangle$ direction. The dHvA signals have been observed just above the superconducting upper critical field $H_{C2} \sim 36.5$ kOe, indicating also the high quality of the sample. Figure 2(a) shows the angular dependences of dHvA frequencies both in the (010) plane and the $(1\bar{1}0)$ plane. The calculated dHvA frequencies are shown in Fig. 2(b), the description of which is given later. In the experiment, six fun-

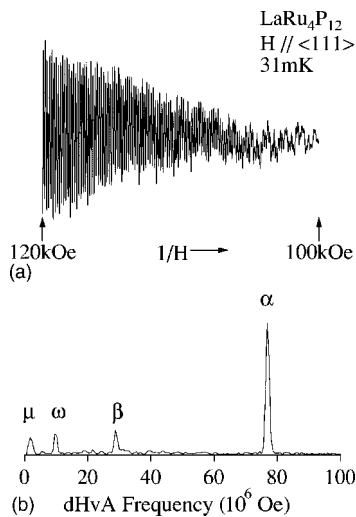


FIG. 1. (a) Typical dHvA oscillations and (b) its fast Fourier transformation (FFT) spectrum in $\text{LaRu}_4\text{P}_{12}$.

fundamental dHvA branches labeled α , β , ω , δ , ε , and μ have been observed. The largest frequency branch α is observed over the whole field angles both in the (010) plane and the (110) plane, although it is not perfectly continuous. The β , ω , and μ branches are observed in the limited angular range around the [111] direction. The δ branch is observed in a narrow angular range centered at the [001] direction. The ε branch is observed in a wider angular range in the (010) plane except near [100].

We have measured the transverse magnetoresistance (TMR), $\Delta\rho/\rho = [\rho(H) - \rho(0)]/\rho(0)$, in $\text{LaRu}_4\text{P}_{12}$ to confirm the existence of an open orbit on the FS. Figure 3 shows the field dependence of TMR for the field along the [100] and [101] directions and the inset shows the angular dependences of TMR under the constant fields in the (010) plane. As was also observed in $\text{LaFe}_4\text{P}_{12}$,¹⁵ the angular dependence of TMR in $\text{LaRu}_4\text{P}_{12}$ is highly anisotropic, suggesting the existence of an open orbit. Actually, as shown later, we have observed the multiply connected (48th band) hole FS in $\text{LaRu}_4\text{P}_{12}$, which is similar to that of $\text{LaFe}_4\text{P}_{12}$. $\text{LaRu}_4\text{P}_{12}$ is an uncompensated metal with a different carrier concentration of electrons and holes, since it has one molecule per unit cell. If

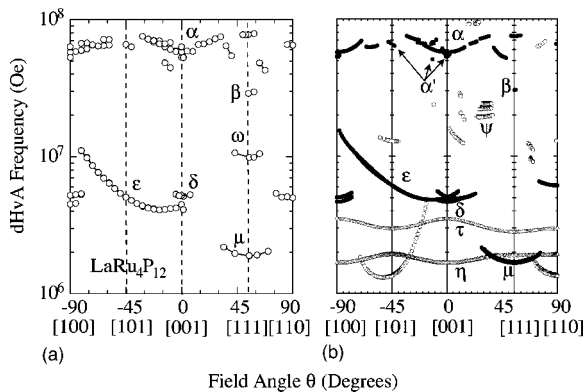


FIG. 2. Angular dependence of the (a) experimental and (b) theoretical dHvA frequencies in $\text{LaRu}_4\text{P}_{12}$. The dHvA branches indicated by the closed marks in (b) are identified by the experiments.

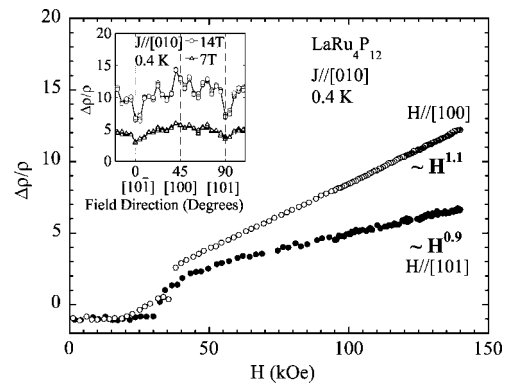


FIG. 3. Magnetic field dependence of the transverse magnetoresistance (TMR) for H along the [100] and [101] directions. The inset shows the angular dependence of TMR under the constant fields of 7 T and 14 T in the (010) plane.

TMR increases with the field, then an open orbit exists for the direction perpendicular to both the current and field. In the present experiment for $H \parallel [100]$, TMR increases with $H^{1.1}$, suggesting the existence of an open orbit.

In order to assign the origin of dHvA branches, the band-structure calculation has been performed by using the full potential linearized augmented-plane-wave (FLAPW) method with the local-density approximation (LDA). We used the room-temperature lattice constant $a = 8.0608 \text{ \AA}$ and the fractional coordinates of P at the 24g site as $x = 0$, $y = 0.3594$, and $z = 0.1434$ for the calculation.²¹ The details of the calculation are essentially the same as in Ref. 15. Figures 4 and 5 show the calculated energy band structure and the FS in $\text{LaRu}_4\text{P}_{12}$, respectively. The FS is composed of the 46th, 47th, and 48th band hole sheets. The main difference with the FS of $\text{PrRu}_4\text{P}_{12}$ is the existence of the 46th and 47th small hole sheets in $\text{LaRu}_4\text{P}_{12}$, while $\text{PrRu}_4\text{P}_{12}$ has only a multiply connected 49th band hole-FS sheet with one band counted for two localized $4f$ electrons.¹⁶ The 46th and 47th bands form nearly spherical sheets centered at the Γ point, which stretch slightly along the $\langle 111 \rangle$ and $\langle 100 \rangle$ directions, respectively. The 48th band gives a multiply connected hole-FS sheet centered at the Γ point. Its shape is roughly a round cube whose volume is nearly one-half of the BZ size and has a good nesting vector $\mathbf{q} = (1, 0, 0)$ as expected also in the 49th band FS of $\text{PrRu}_4\text{P}_{12}$.

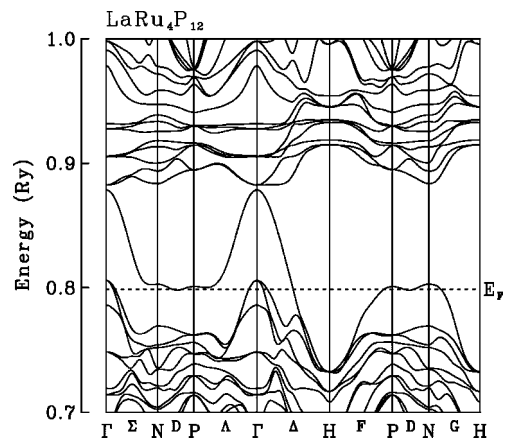


FIG. 4. Energy band structure of $\text{LaRu}_4\text{P}_{12}$.

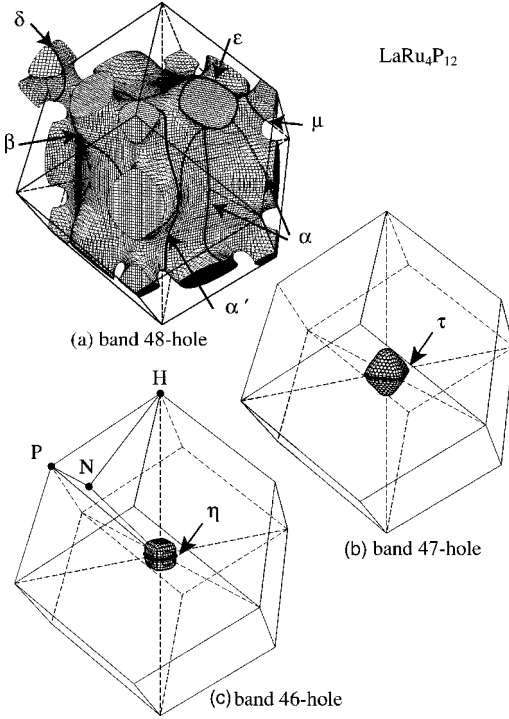


FIG. 5. The Fermi surface of $\text{LaRu}_4\text{P}_{12}$. The estimated volumes of the τ and η band FSs are $\sim 0.3\%$ and $\sim 0.2\%$ of the BZ, respectively.

The calculated dHvA frequencies, shown in Fig. 2(b), reasonably reproduce the angular dependence of the observed dHvA branches α , β , δ , ϵ , and μ , except ω . The α' branch is found to originate from the electronlike orbits in the 48th band FS. The other dHvA branches predicted in the band-structure calculation have not been observed in the present experiments, and the probable origin of this discrepancy is discussed later. We have also estimated the cyclotron effective mass m_c^* from the temperature dependence of the dHvA amplitude. The comparison of dHvA frequencies and m_c^* between the experiment and calculation is given in Table I. The effective mass in the experiment is enhanced roughly twice compared with the calculated one, which is consistent with the enhancement of the Sommerfeld coefficient (γ) between

TABLE I. Comparison of the dHvA frequency F and cyclotron effective mass m_c^* between the experiment and the band-structure calculation in $\text{LaRu}_4\text{P}_{12}$.

Field direction	Branch	Experiment		Theory	
		$F(\times 10^7 \text{Oe})$	m_c^*/m_0	$F(\times 10^7 \text{Oe})$	m_c^*/m_0
$H\parallel[100]$	α	5.81	2.9	5.73	1.87
	δ	0.51	3.9	0.47	2.34
$H\parallel[110]$	α'	6.40		6.65	4.73
$H\parallel[111]$	ϵ	0.50	2.6	0.61	1.40
	α	7.70	9.0	7.50	4.73
	β	2.89	11.8	3.05	3.8
	ω	0.99	3.0		
	μ	0.19	3.2	0.17	1.32

the experiment and the theory.²² Such a large mass enhancement in the La compound is also found in $\text{LaFe}_4\text{P}_{12}$.¹⁵ The large mass enhancement in $\text{LaRu}_4\text{P}_{12}$ should be ascribed to the electron-phonon interaction, taking into account the rather high value of the superconducting transition temperature T_C . Following the McMillan formula with the value of Coulomb pseudopotential $\mu^*=0.13$,²⁴ the Debye temperature $\Theta_D=405$ K, and $T_C=7.3$ K,²² the electron-phonon coupling constant is estimated to be 0.65 in $\text{LaRu}_4\text{P}_{12}$, which is considered as a moderate-coupling superconductor. The value of $\gamma=44.4$ mJ/mol K² and the jump of specific heat at T_C yield the ratio $\Delta C/\gamma T_C \approx 1.58$, which is larger than 1.43 of weak-coupling BCS theory.

The most probable reason why some of the theoretical branches are not observed in the present experiment, particularly for the large dHvA orbits, is a strong reduction of the dHvA signals due to their large curvature factors A'' ($A''=|\partial^2 A/\partial k_H^2|$, where A is the extremal cross-sectional area of the FS and k_H is the wave-vector component along the field direction).²³ The rapid change of A as a function of k_H , i.e., the large value of A'' , diminishes the dHvA amplitude for that extremal area. For the field angle $\theta=30^\circ$: $A''=0.14$ for the α branch whereas $A''=22$ for the ψ branch in the calculation [see Fig. 2(b)]. However, that is not the case for τ and η branches, which originate from the 47th and 46th band FSs, i.e., for $H\parallel[111]$, $A''=0.18$ for the τ branch and $A''=0.61$ for the η branch. The experimental limitations, i.e., insufficient temperatures and magnetic fields, could not be the origin of no observation of τ and η branches, since the μ branch with almost the same curvature factor ($A''=0.4$) and the larger effective mass (see Table I) than those of the τ and η branches (the calculated effective masses for $H\parallel[111]$ are $0.34m_0$ for the τ branch and $0.23m_0$ for the η branch) has been clearly observed. Therefore, dHvA signals should be observed if the τ and η branches really exist. The disagreement between the experiment and calculation concerning the τ and η branches may be ascribed to the small difference of the lattice parameter and/or the effect beyond the LDA treatment. Note that the band-structure calculation shows the absence of the FSs responsible for the τ and η branches in $\text{PrRu}_4\text{P}_{12}$, though the difference of lattice parameter between $\text{LaRu}_4\text{P}_{12}$ (8.0608 Å) and $\text{PrRu}_4\text{P}_{12}$ (8.0424 Å) is quite small ($\sim 0.2\%$).²¹ Thermal expansion measurement suggests that the lattice constant decreases about 1.2% at low temperatures (≤ 20 K) in $\text{LaRu}_4\text{P}_{12}$.²⁵ The band-structure calculation using the low-temperature lattice parameters will be clarified in future work.

From the present dHvA experiment and the band-structure calculation, we have confirmed that the shape of the main FS of $\text{LaRu}_4\text{P}_{12}$ is like a distorted cube [see Fig. 5(a)] and its volume is nearly one-half of the first BZ, indicating the presence of good nesting instability with $\mathbf{q}=(1,0,0)$. The band calculation in $\text{PrRu}_4\text{P}_{12}$ also predicts the nearly perfect FS nesting, leading to the M-I transition.^{16,17} The obtained topology of the main FS in $\text{LaRu}_4\text{P}_{12}$ is similar to that by band calculation in $\text{PrRu}_4\text{P}_{12}$.

Then such a M-I transition should be expected also in $\text{LaRu}_4\text{P}_{12}$, however none has been reported yet; at least the resistivity and specific-heat measurements show no M-I tran-

sition above T_C .²⁶ One can infer that the presence of two small spherical τ and η band FSs predicted by the band calculation, which are absent in $\text{PrRu}_4\text{P}_{12}$, might suppress the M-I transition in $\text{LaRu}_4\text{P}_{12}$. However, the absence of τ and η branches in the present experiment rules out such a scenario with large reliability as mentioned above. In $\text{PrRu}_4\text{P}_{12}$, the change of crystalline structure¹¹⁻¹³ and the marked increase of resistivity below T_{MI} (Ref. 2) are explained by the nesting model, suggesting the disappearance of the entire FS below T_{MI} , based on the band-structure calculations with the localized $4f$ electrons.^{17,18} Note that in $\text{PrFe}_4\text{P}_{12}$, which shows an antiferro-quadrupolar transition below 6.5 K, where only the main part of the FS disappears, the metallic state prevails and heavy fermion behavior appears.⁶⁻⁸ The inelastic neutron scattering (INS) experiment in $\text{PrRu}_4\text{P}_{12}$ shows sharp crystal electric field (CEF) excitation peaks below T_{MI} that gradually broaden across and above T_{MI} ,²⁷ suggesting that the $4f$ electrons are basically localized, though their hybridization with

the conduction electrons (c - f hybridization) increases to some extent across and above T_{MI} . Considering all these facts, naturally, the present experiment suggests an essential $4f$ -electron contribution, which is the main difference between the two compounds, for the M-I transition. The c - f hybridization might cooperate with the FS-nesting condition in causing the M-I transition in $\text{PrRu}_4\text{P}_{12}$, which explains the absence of the M-I transition in $\text{LaRu}_4\text{P}_{12}$ with no $4f$ -electron contribution.

We thank Professor C. Sekine, Professor I. Shirotni, and Professor K. Iwasa for the informative discussion. One of the authors (S.R.S.) acknowledges the support from the Japan Society for the Promotion of Science. This work was partly supported by a Grant-in-Aid for Scientific Research in Priority Area "Skutterudite" (No. 15072204 and No. 15072206) and COE Research (10CE2004) of the Ministry of Education, Culture, Sports, Science and Technology, Japan.

*Electronic address: saha@post.kek.jp; present address: Institute of Material Structure Science, National Laboratory for High Energy Physics (KEK), Tsukuba 305-0801, Japan.

†Present address: Faculty of Integrated Arts and Sciences, Tokushima University, Tokushima 770-8502, Japan.

‡Present address: Dept. of Physics, Okayama University, Okayama 700-8530, Japan.

§Also at Advance Science Research Center, Japan Atomic Energy Research Institute, Tokai, Ibaraki 319-1195, Japan.

¹For a review article, see B. C. Sales, *Handbook on the Physics and Chemistry of Rare Earths*, edited by K. A. Gschneidner, Jr., J.-C. G. Bunzli, and V. K. Pecharsky (Elsevier Science B. V., Amsterdam, 2003), Vol. 33, pp. 1–34.

²C. Sekine, T. Uchiumi, I. Shirotni, and T. Yagi, *Phys. Rev. Lett.* **79**, 3218 (1997).

³E. D. Bauer, N. A. Frederick, P.-C. Ho, V. S. Zapf, and M. B. Maple, *Phys. Rev. B* **65**, 100506(R) (2002).

⁴Y. Aoki, A. Tsuchiya, T. Kanayama, S. R. Saha, H. Sugawara, H. Sato, W. Higemoto, A. Koda, K. Ohishi, K. Nishiyama, and R. Kadono, *Phys. Rev. Lett.* **91**, 067003 (2003).

⁵M. S. Torikachvili, J. W. Chen, Y. Dalichaouch, R. P. Guertin, M. W. McElfresh, C. Rossel, M. B. Maple, and G. P. Meisner, *Phys. Rev. B* **36**, 8660 (1987).

⁶H. Sato, Y. Abe, H. Okada, T. D. Matsuda, K. Abe, H. Sugawara, and Y. Aoki, *Phys. Rev. B* **62**, 15 125 (2000).

⁷Y. Aoki, T. Namiki, T. D. Matsuda, K. Abe, H. Sugawara, and H. Sato, *Phys. Rev. B* **65**, 064446 (2002).

⁸H. Sugawara, T. D. Matsuda, K. Abe, Y. Aoki, H. Sato, S. Nojiri, Y. Inada, R. Settai, and Y. Ōnuki, *Phys. Rev. B* **66**, 134411 (2002).

⁹H. Sugawara, S. Osaki, S. R. Saha, Y. Aoki, H. Sato, Y. Inada, H. Shishido, R. Settai, Y. Ōnuki, H. Harima, and K. Oikawa, *Phys. Rev. B* **66**, 220504(R) (2002).

¹⁰C. Sekine, T. Inaba, I. Shirotni, M. Yokoyama, H. Amitsuka, and T. Sakakibara, *Physica B* **281-282**, 303 (2000).

¹¹C. H. Lee, H. Matsuhara, A. Yamamoto, T. Ohta, H. Takazawa, K. Ueno, C. Sekine, I. Shirotni, and T. Hirayama, *J. Phys.: Condens. Matter* **13**, L45 (2001).

¹²C. H. Lee, H. Matsuhara, H. Yamaguchi, C. Sekine, K. Kihou, and I. Shirotni, *J. Magn. Magn. Mater.* **272-276**, 426 (2004).

¹³L. Hao, K. Iwasa, K. Kuhara, M. Kohgi, S. R. Saha, H. Sugawara, Y. Aoki, H. Sato, C. Sekine, C. H. Lee, and H. Harima, *J. Magn. Magn. Mater.* **272-276**, e271 (2004).

¹⁴S. R. Saha, H. Sugawara, T. Namiki, Y. Aoki, and H. Sato, *J. Phys.: Condens. Matter* **15**, S2163 (2003); S. R. Saha, H. Sugawara, T. Namiki, M. Kobayashi, Y. Aoki, and H. Sato, *J. Magn. Magn. Mater.* **272-276**, e317 (2004).

¹⁵H. Sugawara, Y. Abe, Y. Aoki, H. Sato, M. Hedo, R. Settai, Y. Ōnuki, and H. Harima, *J. Phys. Soc. Jpn.* **69**, 2938 (2000).

¹⁶H. Harima and K. Takegahara, *Physica B* **312-313**, 843 (2002).

¹⁷H. Harima, K. Takegahara, K. Ueda, and S. H. Curnoe, *Acta Phys. Pol. B* **34**, 1189 (2003).

¹⁸S. H. Curnoe, H. Harima, K. Takegahara, and K. Ueda, *Phys. Rev. B* **70**, 245112 (2004).

¹⁹I. Shirotni, T. Adachi, K. Tachi, S. Todo, K. Nozawa, T. Yagi, and M. Kinoshita, *J. Phys. Chem. Solids* **57**, 211 (1996).

²⁰S. R. Saha, H. Sugawara, R. Sakai, Y. Aoki, H. Sato, Y. Inada, H. Shishido, R. Settai, Y. Ōnuki, and H. Harima, *Physica B* **328**, 68 (2003).

²¹C. Sekine (private communication) (these lattice parameters are determined from the recent synchrotron radiation experiment at room temperature).

²²Our recent specific-heat measurement suggests the Sommerfeld coefficient $\gamma \approx 44.4$ mJ/K²mol, while the calculation in the present work gives $\gamma \approx 19.24$ mJ/K²mol.

²³D. Shoenberg, *Magnetic Oscillations in Metals* (Cambridge Univ. Press, Cambridge, 1984), p. 55.

²⁴W. L. McMillan, *Phys. Rev.* **167**, 331 (1967).

²⁵K. Matsuhira, T. Takikawa, T. Sakakibara, C. Sekine, and I. Shirotni, *Physica B* **281**, 298 (2000).

²⁶T. Uchiumi, I. Shirotni, C. Sekine, S. Todo, T. Yagi, Y. Nakazawa, and K. Kanoda, *J. Phys. Chem. Solids* **66**, 689 (1999).

²⁷K. Iwasa, L. Hao, K. Kuwahara, M. Kohgi, S. R. Saha, H. Sugawara, Y. Aoki, H. Sato, T. Tayama, and T. Sakakibara, *Proceedings of SCES2004 [Physica B (to be published)]*.